

Comparison of photodiode nonlinearity measurement systems

Meredith N. Draa,^{1,*} Alexander S. Hastings,² and Keith J. Williams²

¹Global Defense Technology & Systems, Inc., 2200 Defense Highway, Suite 405, Crofton, MD 21114, USA

²Photonics Technology Branch, U. S. Naval Research Laboratory, 4555 Overlook Ave., Washington, DC 20032, USA

*meredith.draa.ctr@nrl.navy.mil

Abstract: Photodiode nonlinearity measurements using one-, two- and three-tone measurement systems are compared with each other, to investigate the comparison accuracy between setups. The mathematical relationship between each setup is analyzed, and data on multiple devices are compared to find under which conditions the measurements are comparable. It is shown that the three measurement systems can be used interchangeably only when the distortion adheres to the expected mathematical slopes.

©2011 Optical Society of America

OCIS codes: (230.5170) Optical devices: photodiodes; (060.2700) Fiber optics and optical communications: radio frequency photonics.

References and links

1. R. D. Esman and K. J. Williams, "Measurement of harmonic distortion in microwave photodetectors," *IEEE Photon. Technol. Lett.* **2**(7), 502–504 (1990).
2. M. N. Draa, J. Ren, D. C. Scott, W. S. Chang, and P. K. L. Yu, "Three laser two-tone setup for measurement of photodiode intercept points," *Opt. Express* **16**(16), 12108–12113 (2008).
3. A. Ramaswamy, J. Klamkin, N. Nnoya, L. A. Johansson, L. A. Coldren, and J. E. Bowers, "Three-tone characterization of high-linearity waveguide uni-traveling-carrier photodiodes," in *21st Annual Meeting of the IEEE Lasers and Electro-Optics Society, 2008. LEOS 2008* (IEEE LEOS, 2008), pp. 286–287.
4. H. Pan, A. Beling, and J. C. Campbell, "High-linearity uni-traveling-carrier photodiodes," *IEEE Photon. Technol. Lett.* **21**(24), 1855–1857 (2009).
5. T. Ohno, H. Fukano, Y. Muramoto, T. Ishibashi, T. Yoshimatsu, and Y. Doi, "Measurement of intermodulation distortion in untraveling-carrier refracting-facet photodiode and a p-i-n refracting-facet photodiode," *IEEE Photon. Technol. Lett.* **14**(3), 375–377 (2002).
6. D. C. Scott, T. A. Vang, J. Elliott, D. Forbes, J. Lacey, K. Everett, F. Alvarez, R. Johnson, A. Krispin, J. Brock, L. Lembo, H. Jiang, D. S. Shin, J. T. Zhu, and P. K. L. Yu, "Measurement of IP3 in p-i-n photodetectors and propose performance requirements for RF fiber-optics links," *IEEE Photon. Technol. Lett.* **12**(4), 422–424 (2000).
7. H. Jiang, D. S. Shin, G. L. Li, T. A. Vang, D. C. Scott, and P. K. L. Yu, "The frequency behavior of the third-order intercept point in a waveguide photodiode," *IEEE Photon. Technol. Lett.* **12**(5), 540–542 (2000).
8. T. Ozeki and E. H. Hara, "Measurement of nonlinear distortion in photodiodes," *Electron. Lett.* **12**(3), 80–81 (1976).
9. A. Famaswamy, N. Nunoya, M. Piels, L. A. Johansson, L. A. Coldren, A. S. Hastings, K. J. Williams, and J. Klamkin, "Experimental analysis of two measurement techniques to characterize photodiode linearity," in *International Topical Meeting on Microwave Photonics, 2009. MWP '09* (IEEE, 2009), pp. 1642–1644.
10. A. S. Hastings, D. A. Tulchinsky, and K. J. Williams, "Photodiode nonlinearities due to voltage-dependent responsivity," *IEEE Photon. Technol. Lett.* **21**(21), 1642–1644 (2009).
11. V. J. Urick, P. S. Devgan, J. D. McKinney, and J. L. Dexter, "Laser-noise and its impact on the performance of intensity-modulated direct-detection analog photonic links," *NRL Memorandum Report, NRL/MR/5652–07–9065*, August 2007.
12. K. J. Williams, L. T. Nichols, and R. D. Esman, "Photodetector nonlinearity limitations on a high-dynamic range 3GHz fiber optic link," *J. Lightwave Technol.* **16**(2), 192–199 (1998).
13. H. Pan, J. C. Campbell, A. Beling, H. Chen, and P. D. Yoder, "A high-linearity modified uni-traveling carrier photodiode with offset effects of nonlinear capacitance," *J. Lightwave Technol.* **27**(20), 4435–4439 (2009).

1. Introduction

Photodiode linearity is an important metric for analog optical links requiring high dynamic range. Nonlinearity measurement in photodiodes has been accomplished using a number of setups usually involving either heterodyning techniques or Mach-Zehnder modulators (MZM)

Report Documentation Page

Form Approved
OMB No. 0704-0188

Public reporting burden for the collection of information is estimated to average 1 hour per response, including the time for reviewing instructions, searching existing data sources, gathering and maintaining the data needed, and completing and reviewing the collection of information. Send comments regarding this burden estimate or any other aspect of this collection of information, including suggestions for reducing this burden, to Washington Headquarters Services, Directorate for Information Operations and Reports, 1215 Jefferson Davis Highway, Suite 1204, Arlington VA 22202-4302. Respondents should be aware that notwithstanding any other provision of law, no person shall be subject to a penalty for failing to comply with a collection of information if it does not display a currently valid OMB control number.

1. REPORT DATE 2011	2. REPORT TYPE	3. DATES COVERED 00-00-2011 to 00-00-2011	
4. TITLE AND SUBTITLE Comparison Of Photodiode Nonlinearity Measurement Systems		5a. CONTRACT NUMBER	
		5b. GRANT NUMBER	
		5c. PROGRAM ELEMENT NUMBER	
6. AUTHOR(S)		5d. PROJECT NUMBER	
		5e. TASK NUMBER	
		5f. WORK UNIT NUMBER	
7. PERFORMING ORGANIZATION NAME(S) AND ADDRESS(ES) Global Defense Technology & Systems, Inc., 2200 Defense Highway, Suite 405, Crofton, MD, 21114		8. PERFORMING ORGANIZATION REPORT NUMBER	
9. SPONSORING/MONITORING AGENCY NAME(S) AND ADDRESS(ES)		10. SPONSOR/MONITOR'S ACRONYM(S)	
		11. SPONSOR/MONITOR'S REPORT NUMBER(S)	
12. DISTRIBUTION/AVAILABILITY STATEMENT Approved for public release; distribution unlimited			
13. SUPPLEMENTARY NOTES Optics Express, 20 June 2011, Vol. 19, No. 13, Government or Federal Purpose Rights License.			
14. ABSTRACT Photodiode nonlinearity measurements using one-, two- and three-tone measurement systems are compared with each other, to investigate the comparison accuracy between setups. The mathematical relationship between each setup is analyzed, and data on multiple devices are compared to find under which conditions the measurements are comparable. It is shown that the three measurement systems can be used interchangeably only when the distortion adheres to the expected mathematical slopes.			
15. SUBJECT TERMS			
16. SECURITY CLASSIFICATION OF:			17. LIMITATION OF ABSTRACT
a. REPORT unclassified	b. ABSTRACT unclassified	c. THIS PAGE unclassified	Same as Report (SAR)
			18. NUMBER OF PAGES 11
			19a. NAME OF RESPONSIBLE PERSON

to create fundamental RF tones modulated on the optical input [1–9]. Harmonic distortion is measured using a pure RF-modulated optical signal incident on the photodiode, which generates photodiode-induced harmonics in addition to a fundamental tone. The measured powers of the fundamental and harmonic tones can then be extrapolated as a function of input RF power to calculate the second- and third-order harmonic output intercept points (OIP_{2it} and OIP_{3it} respectively). Intermodulation distortion is measured using multiple tones to induce mixing at the sum and difference frequencies of the fundamental tones. Again, OIP values can be determined by extrapolating the measured RF powers of the distortion and fundamental.

Previous work has detailed theoretical mathematical relationships between different setups [3,5,9], however there has been no study to determine when these relationships are physically true in photodiode operation. The mathematical relationships make various assumptions (i.e. memoryless, well behaved nonlinearities operating under sinusoidal input) that may not always hold true in every case for every device. The nonlinearities generated from harmonic and intermodulation distortion are still largely not understood- numerous authors have presented arguments for various possible causes [4,7,10], but little has been done to explore the consistency between various measurement setups. The aim of this work is to present three setups used to measure photodiode distortion, develop the mathematical relationships that allow the comparison of OIP across all measurement setups and measure multiple photodiodes to determine when the OIP is consistent between setups.

With a multitude of setups that are used to measure nonlinearities, there has been no comprehensive study of possible discrepancies between each measurement system and the conditions under which each system accurately measures photodiode distortion. Considering the two-tone MZM setup, Draa et al. showed that distortion caused by the MZMs could introduce additional nonlinearities into the measurement, making it inaccurate when using the traditional setup [2]. Ramaswamy et al. proposed using a three-tone MZM setup to eliminate the contribution of modulator-induced distortion to the measured third order intermodulation distortion, using mathematical conversions to relate the measured data to the two-tone setup. The three-tone setup provided higher OIP_3 results under certain conditions, leading the authors to conclude that the three-tone setup is the measurement system with less chance of MZM nonlinearities directly interacting with the photodiode nonlinearities at high OIP_3 levels [9]. However, the accuracy of the comparison relies on the mathematical relationship between the two- and three-tone measurements. If this relationship cannot be experimentally verified, the results of the two setups cannot be compared. Additionally, Pan et al. measured devices using both the two-tone and three-tone MZM setups and showed little measurement differences between them with their device even at high OIP_3 values ($\sim 50\text{dBm}$) [4]. The heterodyning technique has been touted for its lack of additionally contributed nonlinearities, but is generally considered to be the most complex of the setups, and has never been directly compared to modulator measurements [6].

In all the works mentioned, there is no consensus as to which measurement system provides the most accurate results, and whether the data from one setup can be equivalently measured using another. The purpose of this work is to measure photodiode distortion using the three widely used setups at a range of bias voltages and modulation depths; the three-tone MZM and the one- and two-tone heterodyne setups will be used to measure photodiode distortion in order to compare nonlinearity data from each setup. The results will determine under which circumstances the theoretical mathematical relationships can be applied to each setup.

2. Measurement setups

The five-laser heterodyne setup can be seen in Fig. 1. There are two pairs of Lightwave Electronics LWE-125 diode pumped Nd:YAG lasers operating at a 1319nm optical wavelength. The optical offset frequency for each pair is stabilized by mixing the resulting RF intermodulation tone ($\lambda_{1/3}-\lambda_{2/4}$) with an RF reference signal and running the mixed product through a phase-locked loop (PLL) amplifier circuit back into the piezo-electric wavelength

control for one of the lasers. Each output is fed through an optical attenuator and then combined using a 50/50 optical coupler and combined with a 5th laser (Nd:YAG) used to control the average photodiode (PD) current. The device under test (DUT) is illuminated with the resulting signal and the RF output power is measured by an electrical spectrum analyzer (ESA). The modulation index is changed by attenuating each pair of heterodyned lasers, and adjusting the attenuation of the 5th laser (λ_5) to compensate so that the total photocurrent is kept constant. In this setup, the wavelengths of the lasers must be carefully controlled so that all unwanted optical intermodulation tones in the RF frequency domain fall outside the bandwidth of the photodiode under test. The tuning range of the LWE-125 laser is about 40GHz, so each set of heterodyned lasers and the DC laser were each tuned to be 20GHz from each other, far outside the 3GHz bandwidth of the detector. The signal produced is stable enough that measurements can be taken with a 10Hz resolution bandwidth (RBW), and averaging the results over a 30 second span with no movement of the fundamental or harmonics. The single-tone setup is configured by completely turning off one pair of heterodyned lasers.

Figure 2 shows the three-tone MZM setup. Three Lightwave Electronics model-125 diode pumped Nd:YAG lasers are modulated by three MZMs and fed through optical attenuators. The first two lasers are combined using a 50/50 coupler, and then to the third with another 50/50 coupler. Finally, an unmodulated Nd:YAG laser is input to an optical attenuator and combined with the signal using a 50/50 coupler. The output is fed into the DUT, and the RF output is measured by an ESA (Agilent E4440A) using a 10Hz RBW and VBW with a 1KHz span. The noise floor is -140dBm with averaging, which gives a minimum detectable nonlinearity of -120dBm because of a 20dB RF pad in front of the ESA. The MZM setup utilizes similar laser wavelengths as the heterodyne setup to remove measurement differences resulting from optical wavelength dependencies of the photodiode under test. For all measurements, 20dB attenuation was required between the bias tee and the ESA to insure that the distortion produced in the ESA was below that of the PD.

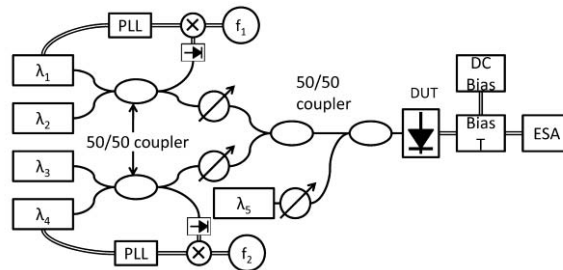


Fig. 1. Five laser two-tone heterodyne setup

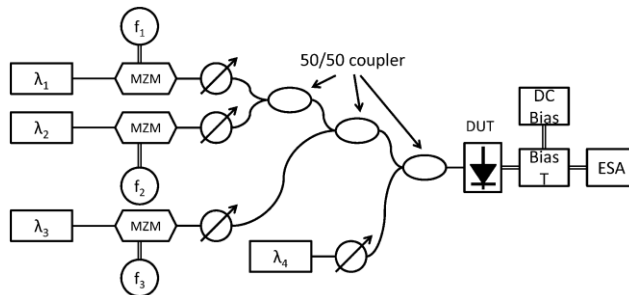


Fig. 2. Four laser three-tone MZM measurement setup

Both of these setups were designed to minimize the contribution of any distortion produced by the measurement system on the measured photodiode nonlinearity. In the five laser two-tone heterodyne setup, additional tones will be produced at $\lambda_{1/3} + \lambda_{2/4}$, but this value

will be far above the bandwidth of the detector. In the four laser three-tone MZM setup, second and third order distortion terms will be produced which have only F1, F2 and F3 terms contributing, with no multiples of the fundamental, such as 2·F1-F2. This removes the chance of any second harmonics of the fundamentals contributing to a third order distortion product. In both setups, we can be certain that nonlinearity contributed by the measurement system is minimized.

3. Mathematical relationships

To determine the mathematical relationship between the data from each setup, a generalized photodiode responsivity nonlinearity, \mathfrak{R} , will be designated. We can express photocurrent as a function of optical power by:

$$I = P(t)\mathfrak{R}(x) \quad (1)$$

We will define $\mathfrak{R}(x)$ as a nonlinear transfer function of a physical variable x that can be approximated using a Taylor series around some arbitrary value, a , up to the second order:

$$\mathfrak{R}(x) \approx \mathfrak{R}(a) + \mathfrak{R}'(a)(x-a) + \frac{\mathfrak{R}''(a)}{2}(x-a)^2 \quad (2)$$

The incident optical power in each setup will be defined by a sum of sinusoids,

$$P(t) = P_{avg} \left[1 + \left(\sum_{l=1}^k m_l \sin(\omega_l t) \right) \right] \quad (3)$$

where $k=1$ for the one-tone heterodyne, $k=2$ for the two-tone heterodyne and $k=3$ for the three-tone MZM setup, P_{avg} is the average power, m_l is the modulation index, and ω_l is the RF tone frequency. In the heterodyne setup, m_l can be determined by simply measuring the average power contributions from each of the heterodyned laser pairs and the DC laser. In the modulator setup, m_l can be calculated using the RF input power to the modulator, optical input power, and modulator transfer function [11]. We can assume x is some slowly varying function of $P(t)$ and that small signal conditions apply so that:

$$x \approx \delta \cdot P(t) \quad (4)$$

where δ is some constant. Substituting Eq. (4) and Eq. (2) into Eq. (1) we have:

$$I = c_1 P(t) + c_2 P^2(t) + c_3 P^3(t) \quad (5)$$

where $c_1 = \mathfrak{R}(a) - \mathfrak{R}'(a)a + \frac{\mathfrak{R}''(a)}{2}a^2$, $c_2 = \mathfrak{R}'(a)\delta - 2\frac{\mathfrak{R}''(a)}{2}\delta a$, and $c_3 = \frac{\mathfrak{R}''(a)}{2}\delta^2$. For a one-tone signal where $l=1$, we can substitute the expanded form of Eq. (3) into Eq. (5).

$$I = P_{avg} \left\{ c_1 \left[1 + m_1 \sin(\omega_1 t) \right] + c_2 \left[1 + 2m_1 \sin(\omega_1 t) + \frac{m_1^2}{2}(1 - \cos(2\omega_1 t)) \right] + c_3 \left[1 + 3m_1 \sin(\omega_1 t) + \frac{3m_1^2}{2}(1 - \cos(2\omega_1 t)) + \frac{m_1^3}{4}(3\sin(\omega_1 t) - \sin(3\omega_1 t)) \right] \right\} \quad (6)$$

From Eq. (6), the coefficients for the fundamental, second order and third order components can be extracted. Repeating this series of steps for $k=2$ and 3 , the resulting intermodulation and harmonic terms in each measurement system can be isolated and compared with each other. This small signal approximation comparison holds for any well-behaved single

photodiode nonlinearity, so that for every dB increase in the fundamental, the n^{th} order distortion increases by n dB.

When the one-, two- and three-tone cases are compared with each other, similar ordered distortion in each case can be compared while keeping the modulation index constant. The second order relationships using the two-tone setup as the basis, are described by

$$HD2_{1t} + 6 = IMD2_{2t} = IMD2_{3t} \text{ (dBm)} \quad (7)$$

where $HD2_{1t}$ is the second order harmonic distortion for the one-tone setup and $IMD2_{2t}$ and $IMD2_{3t}$ are the second order intermodulation distortion for the two-tone and three-tone setups respectively [12]. For the third order distortion, the relationships using the two-tone setup as the base, are described by

$$HD3_{1t} + 9.54 = IMD3_{2t} = IMD3_{3t} - 6 \text{ (dBm)} \quad (8)$$

where $HD3_{1t}$, $IMD3_{2t}$ and $IMD3_{3t}$ are the third order distortion for the one-, two- and three-tone setups respectively [12]. Finally, the relationship between OIP2 and OIP3 for each setup can be determined by,

$$OIP2 = 2F - IMD2 \text{ (dBm)} \quad (9a)$$

$$OIP3 = \frac{3}{2}F - \frac{1}{2}IMD3 \text{ (dBm)} \quad (9b)$$

where F is the average power of the fundamentals, in dBm, and $IMD2/IMD3$ can also be the harmonic distortion ($HD2/HD3$) of the one-tone setup. Using Eq. (9a), the relationship between OIP2, using the two-tone setup as the base is

$$OIP2_{1t} - 6 = OIP2_{2t} = OIP2_{3t} \text{ (dBm)} \quad (10)$$

Similarly, using Eq. (9b) the relationship between OIP3 using the two-tone setup as the base, in dBm units of power, is

$$OIP3_{1t} - 4.77 = OIP3_{2t} = OIP3_{3t} + 3 \text{ (dBm)} \quad (11)$$

Using Eq. (10) and Eq. (11), the data from the one- and three-tone measurement systems can be shifted according to the constants so that comparisons between the three systems can be made.

4. Results and analysis

4.1 Applied Electronics PD3000

A 3GHz-bandwidth photodiode (Applied Electronics model: PD3000) was measured. The measurement was taken around a 100MHz center frequency with 10MHz spacing for the two- and three-tone setups, at 10mA average photocurrent. The tones were set to slightly offset frequencies (i.e. 89.59MHz instead of 90.00MHz) instead of integers to avoid any extraneous signals present in the environment that might mix and add to distortion at even numbers (i.e. 10MHz, 100MHz). All second and third order distortion products were measured as a function of photodiode bias voltage and modulation depth. In general practice, OIP is extracted by plotting the fundamental and second and third order distortion as a function of modulation depth or input power and then fitting each with a slope of one, two, and three respectively according the mathematical relationships established in section 3. Assuming this is the case, local OIP2 and OIP3 were calculated at each bias voltage point using Eq. (9a) and Eq. (9b) for the same modulation depth across each setup. The data were plotted at the same input modulation depth across all setups to get the most accurate local OIP2 and OIP3 comparison between setups.

Figure 3 shows the OIP2 versus bias voltage for all second order distortion in the three setups separated into areas A and B. The plot contains the second order intermodulation distortions that add (i.e. $F1 + F2$) as well as those that subtract (i.e. $F2-F1$). The one-tone heterodyne setup provides the second order harmonic ($2 \cdot F1$) at 200MHz. To compare the three measurement setups, the $OIP2_{1t}$ and $OIP2_{3t}$ data are shifted according to Eq. (10) to $OIP2_{2t}$. The three measurement setups are designated by color, red for the one-tone, blue for the two-tone, and green for the three-tone. The color scheme for each setup will be maintained throughout the remaining figures. At low bias voltages (area A), the data clearly line up for low frequency (solid points) and high frequency (open points) distortion. At high bias voltages (area B), the data at high frequencies for the three-tone setup remain consistent. There is a large divergence between all three setups from 5 to 6V. For the low frequency distortion at high voltages, $F3-F1$ and $F3-F2$ for the three-tone setup merge together along with $F2-F1$ of the two-tone, where before $F3-F1$ was significantly lower than the distortion closer to 10MHz. The difference between the low and high frequencies will be addressed later.

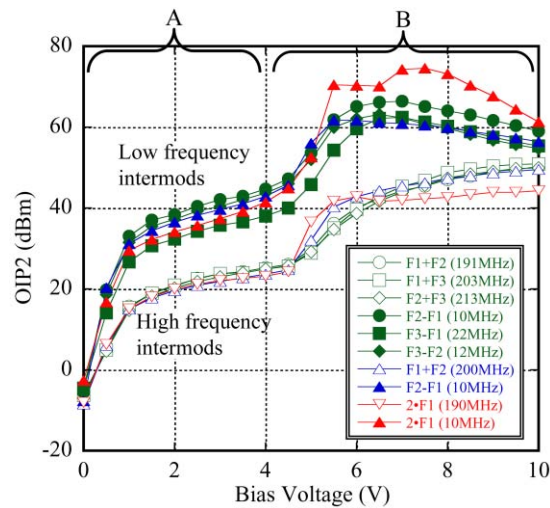


Fig. 3. OIP2 versus bias voltage for a PD3000 photodiode, using one-, two- and three-tone measurement setups. Fundamental frequency $f = 100\text{MHz}$, with frequency spacing $\Delta f = 10\text{MHz}$ and total photocurrent = 10mA. One- and three-tone data are shifted according to Eq. (10) to mathematically match the two-tone data. One-tone data for 5MHz fundamental included (red solid triangles).

In Fig. 4, OIP3 is plotted versus bias voltage from 0 to 10V for intermods with frequencies close to the fundamental frequency. In this instance the MZM setup contributes three sets of data, $F1 + F2-F3$, $F1-F2 + F3$, and $F2 + F3-F1$, while the two-tone heterodyne setup contributes data for $2 \cdot F1-F2$ and $2 \cdot F2-F1$. To compare the data sets from each measurement setup, the one- and three-tone data are shifted as per Eq. (11), to compare them to the two-tone setup. In Fig. 4, the data match up well in area A ($\pm 1\text{dB}$). In area B, the two-tone setup and three-tone setup no longer overlap. Also, the different OIP3 values within each setup begin to deviate from each other. For the three-tone setup there is about 1dB between each data set, with the OIP3 decreasing as the frequency of the distortion increases (78MHz, 102MHz, and 122MHz). For the two-tone setup, the data cross back and forth with no clear pattern. The largest discrepancy between the measurement systems is 8dB corresponding to a 16dB difference in distortion, which is quite substantial.

Similarly, the OIP3 data for intermods close to the third harmonic frequency are plotted in Fig. 5. The three-tone setup provided $F1 + F2 + F3$, the two-tone $F1 + 2 \cdot F2$ and $2 \cdot F1 + F2$, and the one-tone $3 \cdot F1$. The data match well in area A as in Fig. 4; however the three setups begin to diverge at higher bias voltages in area B as seen before in Figs. 3 and 4. After 5V

there is a large divergence from any pattern in the data. The one-tone data in particular are much lower than the other two setups.

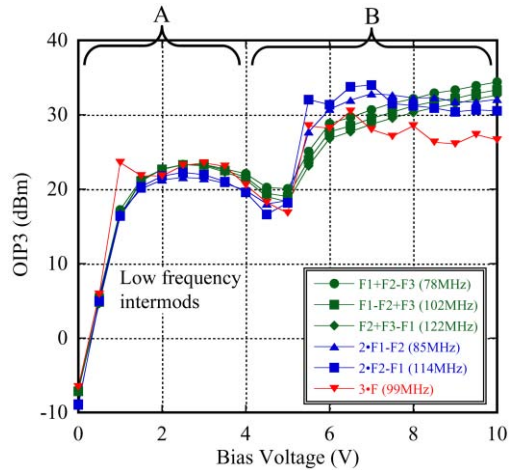


Fig. 4. OIP3 versus bias voltage for a PD3000 photodiode, using one-, two- and three-tone measurement setups. Fundamental frequency $f = 100\text{MHz}$, with frequency spacing $\Delta f = 10\text{MHz}$ and total photocurrent = 10mA . Only distortion near f is plotted. One- and three-tone data are according to Eq. (11) to mathematically match the two-tone data. One-tone data for 33MHz fundamental included (red solid triangles).

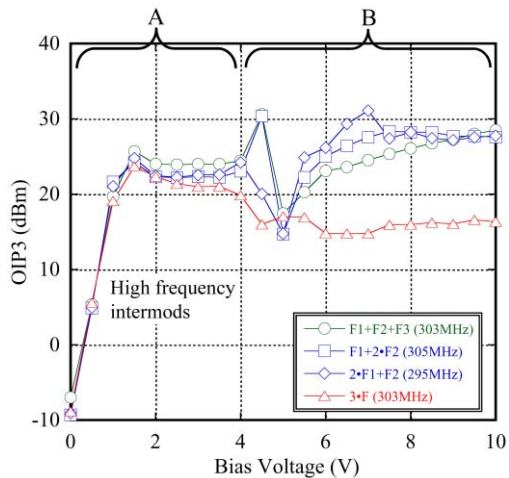


Fig. 5. OIP3 versus bias voltage for a PD3000 photodiode, using one-, two- and three-tone measurement setups. Fundamental frequency $f = 100\text{MHz}$, with frequency spacing $\Delta f = 10\text{MHz}$ and total photocurrent = 10mA . Only distortion near $3 \cdot f$ is plotted. One- and three-tone data are according to Eq. (11) to mathematically match the two-tone data.

The OIP3 data are plotted separately for low (near the fundamental) and high frequency cases (near 3 times the fundamental) because the shapes of the curves do not match up at the two sets of frequencies (similar to the OIP2 case). In the second order case, the low frequency OIP2s (around 10MHz) are significantly higher than the high frequency OIP2s. The OIP2 that results in double the frequency spacing ($\sim 20\text{MHz}$) is slightly lower than the 10MHz OIP2s. In general, the low frequency cases have less distortion (and therefore a higher OIP) than the high frequency cases. This frequency dependence appears to be more pronounced at low frequencies (around 10MHz) than at high frequencies (around 200MHz). Therefore, there is a significant difference in OIP2 between $F2-F1(10\text{MHz})$ and $F3-F1(20\text{MHz})$ for the three-tone

case, with a separation of 10MHz. With similar separation at high frequencies there is no difference in OIP2 for F1 + F2 (191MHz) and F1 + F3 (203MHz). The disparity between same order distortion, as a function of frequency leads to the conclusion there is some frequency dependence within a certain order of photodiode nonlinearity.

Additional data are plotted in Figs. 3 and 4 to analyze this frequency dependence. The OIP2 from the one-tone setup (red solid triangles) with a 5MHz fundamental resulting in a second order harmonic at 10MHz is plotted in Fig. 3. In area A, the data line up well with the low frequency data from the two- and three-tone setups, despite originating from a much lower fundamental frequency. Data are plotted in Fig. 4 from the one-tone setup (red solid triangles) with a fundamental of 33MHz, which results in a third order harmonic at 99MHz. The data match well with the other nonlinearities around 100MHz in area A. Again, in both cases, the harmonic distortion deviates at higher bias voltages in area B. The general patternless deviation of all distortion at higher bias voltage is probably a result of nonlinearity characteristics specific to this photodiode, since we also observed photodiodes where the distortion matches up well at high bias voltages.

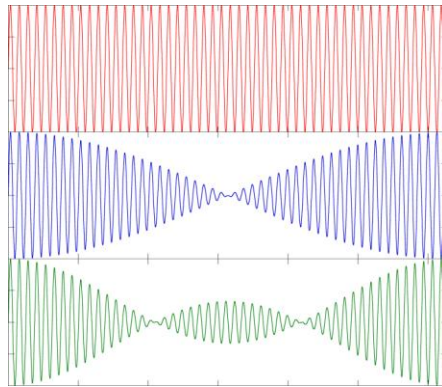


Fig. 6. Plots of the electric field vs. time for one-tone (top), two-tone (middle) and three-tone (bottom) measurements.

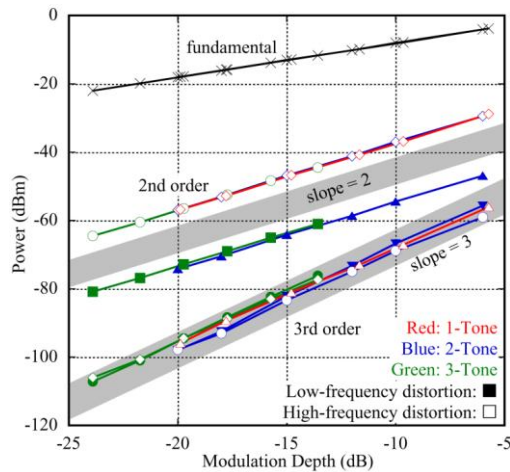


Fig. 7. Fundamental and selected second and third order distortion power versus modulation depth at 2.5V bias for a PD3000 photodiode. Fundamental frequency $f = 100\text{MHz}$, with frequency spacing $\Delta f = 10\text{MHz}$ and total photocurrent = 10mA. One- and three-tone data are according to Eq. (10) and Eq. (11) to mathematically match the two-tone data.

The large difference in low and high frequency second order distortion values can be attributed to the differences in electric field that the diode sees between the measurement

systems. The plots of the electric field for the one-tone, two-tone and three-tone sinusoidal measurement systems are shown in Fig. 6. The data in Fig. 3 and Fig. 4 from the one-tone setup at different fundamentals (5MHz and 33MHz) demonstrate that the OIP2 and OIP3 are not necessarily a strong function of the fundamental frequencies. Instead the nonlinearity may be a function of the time dependent envelopes of the electric field rather than from the higher frequency. Since low frequency nonlinearity is dependent on the envelope frequency, and the high frequency nonlinearity is dependent on the internal “carrier” frequency, the resulting distortion levels will differ to reflect the large difference in frequency they originate from.

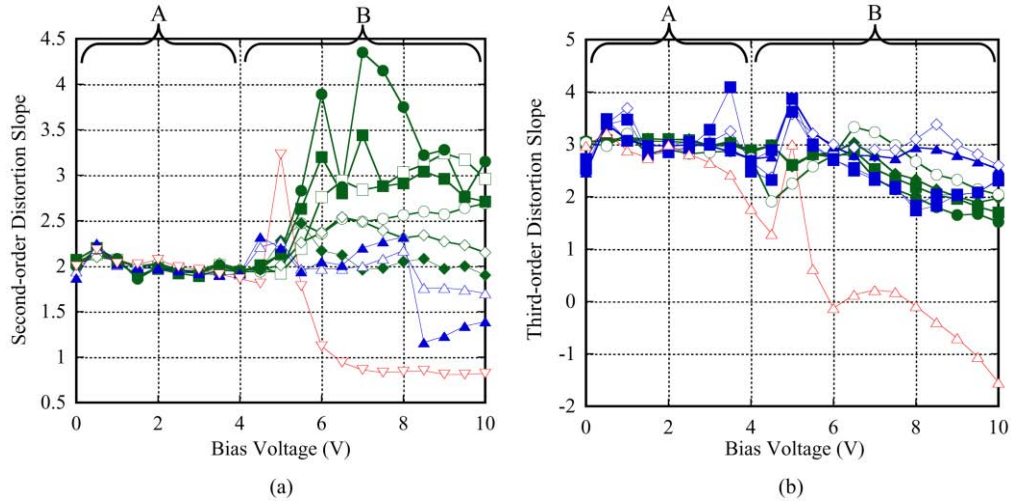


Fig. 8. Slope of (a) IMD2/HD2 and (b) IMD3/HD3 vs. bias voltage for PD3000 for all three setups.

Now that the diode has been analyzed over a range of bias voltages to determine the correlation of the setups, the relationship of the output RF power and modulation depth can be discussed. In Fig. 7, fundamental, second and third order distortion power is plotted versus modulation depth at 2.5V bias, corresponding to area A in Figs. 3-5, where the data from the different setups were well-correlated. Again, the one- and three-tone distortion second and third order distortion data have been shifted to the two-tone setup, as per Eq. (7) and Eq. (8) respectively. In the plot, the second order data clearly line up for low and high frequencies over the entire measured range of modulation depths. Additionally the data are all within 3% deviation of the expected slope value of two. The slopes of the 3rd order distortion are similarly behaved (slope of three) across all measurement setups. All of the data agree to within ± 1 dB at different modulation depths, indicating that all setups are measuring the same nonlinearity, and therefore producing the same local OIP. In this case, we conclude that the measurement setups can be used interchangeably since the mathematical relationships in Eq. (10) and Eq. (11) hold true. To illustrate the desired measurement behavior more clearly, the slopes of the measured IMD2/HD2 and IMD3/HD3 are plotted vs. bias voltage in Fig. 8a and Fig. 8b respectively. The slopes match up to 2 very well up in area A in Fig. 8a. In Fig. 8b there is some discrepancy at 0.5V, 1V and 3.5V, but the general trend does not diverge until higher voltages in area B. The larger error in the slope values for the third order distortion is attributed to fact that the third order distortion is a more complex process than the second order, and thus is not as consistent with the ideal theoretical behavior. When the slopes diverge significantly from their expected values, OIP becomes impossible to calculate, and Eq. (10) and Eq. (11) are no longer useful in comparing the three setups. For Figs. 3-5 this makes the OIP values for bias voltage higher than 4V invalid.

4.2 Additional Devices

In order to confirm that the behavior in 4.1 is not a singular case for the diode tested, two other devices were measured using the three setups. A second commercial diode from Applied Electronics (Model: PD1000) was tested at 10mA at a center frequency of 100MHz with 10MHz spacing from 0 to 10V bias. The PD1000 is similar to the PD3000, but has a bandwidth of 1GHz instead of 3GHz. The OIP2 vs. bias voltage is plotted in Fig. 9a. The OIP2 is similar to that of the PD3000 in Figs. 4 and 5, where the setups match up well in area A. The slope of the distortion is plotted in Fig. 9b where the slope is close to 2 in area A, but exhibits more discrepancy than in the PD3000 case, particularly at 0.5V, where all frequencies show a spike in slope. The OIP3 for the PD1000 was also measured and exhibited similar behavior to the PD3000 and is thus not graphed. As before in area B the OIP2 diverges, meaning the OIP2 cannot be extracted as the slopes do not match the mathematical values.

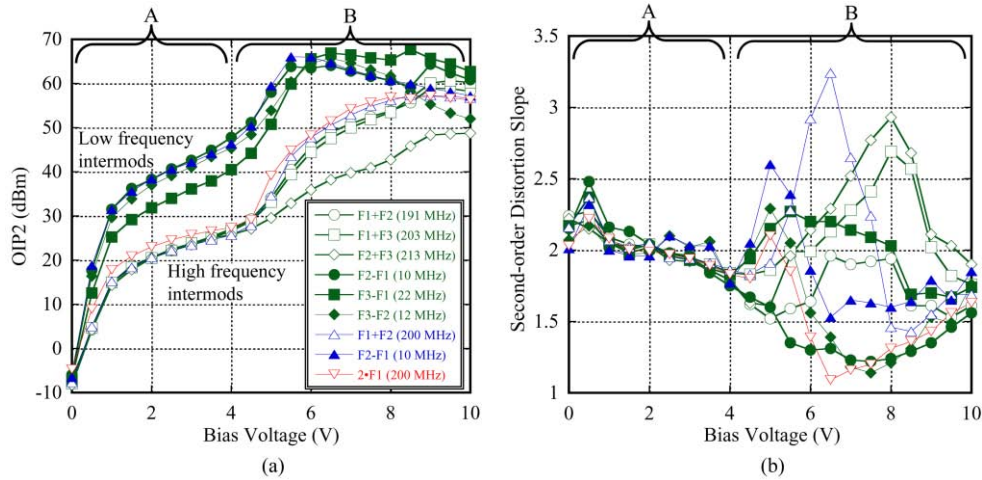


Fig. 9. (a) OIP2 vs. bias voltage for PD1000 at center frequency 100MHz with 10MHz spacing at 10mA photocurrent for one-, two- and three-tone setups and (b) IMD2/H23 slope vs. bias voltage for PD1000. In (a), one- and three-tone data are according to Eq. (10) to mathematically match the two-tone data.

A third commercial device was measured that was not from Applied Electronics, which will be referred to as Device C and has a bandwidth of 20GHz. Device C was measured at the same conditions as the PD3000 in section 4.1. The OIP2 vs. bias voltage is plotted in Fig. 10a. In this case, OIP2 at all distortion frequencies matches well in area B, at higher bias voltages, but is inconsistent in area A, at lower voltages. To confirm if the same conditions used previously apply, the slope of the second order distortion is plotted in Fig. 10b. It is clear that the slopes are all approximately 2 in area B, where the OIP2 matches well between all setups, whereas in area A the slopes do not match up and therefore the OIP2 extracted is invalid according to the mathematical definition. Since for Device C the setups produce consistent results at a different range of voltages than for the PD3000 and PD1000, there is unlikely to be a general explanation for the discrepancy of distortion slope from its expected value. We can conclude that nonlinearity measurements made on different setups cannot be cross compared unless the distortion produces the correct theoretical slope vs. modulation depth, and in order to verify the slope, detailed distortion measurements as a function of modulation depth must be made. Deviation of the distortion slope from the expected value could be caused by several factors in the photodiode. Nonlinearities identified previously in [4,7,10], may provide higher order terms that dominate at a lower order distortion, and phasing/de-phasing between two competing nonlinearities can cause cancellation [13] in the distortion measurement. In the mathematical model, the assumption was made that high order terms would not dominate; however slopes higher than the ideal value suggest the higher order

nonlinearities should be investigated both mathematically, by expanding the Taylor series, and experimentally in the future.

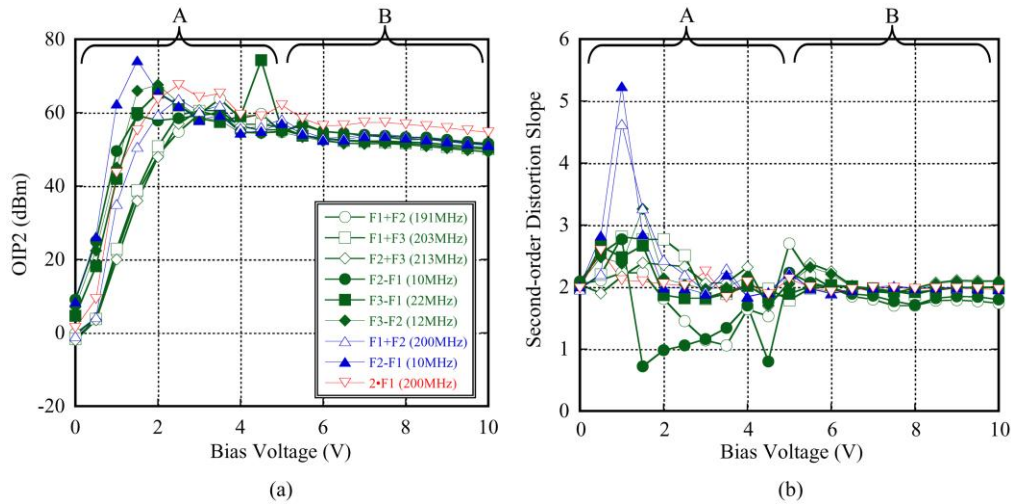


Fig. 10. (a) OIP2 vs. bias voltage for Device C at center frequency 100MHz with 10MHz spacing at 10mA photocurrent for one-, two- and three-tone setups and (b) IMD2/HD2 slope vs. bias voltage for Device C. In (a), one- and three-tone data are according to Eq. (10) to mathematically match the two-tone data.

5. Conclusion

Nonlinearity was measured (OIP2 and OIP3) for the PD3000 photodiode using three setups, a one-tone heterodyne, two-tone heterodyne and three-tone MZM design. The data from each setup were measured over a range of 10V bias voltage with a 100MHz center frequency and 10MHz separation between tones. The results matched well between all setups from low bias voltages, where the diode exhibited the expected behavior versus modulation depth, verifying the mathematical relationships developed in section 3. At higher bias voltages, the results diverged for each setup and were no longer correlated to each other. The slopes versus modulation depth no longer adhered to the mathematical relationships of two for OIP2 and three for OIP3, invalidating the three setups as consistent measurements. Data were also taken using the one-tone setup demonstrating a nonlinearity correlation resulting from the frequency at which the distortion occurs, as opposed to the frequency of the fundamental. Additionally, data were taken on two other devices, in which the theoretical mathematical relationship requirement confirmed the consistency of the different setup measurements. We have shown that while all three measurements systems are capable of producing accurate nonlinearity measurements, they do not do so under all circumstances. In order to insure the accuracy of the measurement, more than a “spot” check of OIP at a single modulation depth is needed. Even in the absence of setup nonlinearity (MZM nonlinearity), device nonlinearities such as higher order distortion products or possible phase cancellation between competing mechanisms can affect the measured slope as a function of modulation depth, making the extraction of OIP impossible per the mathematical definition. From our data, we can assume that as long as the slopes of the nonlinearities match their expected values over a range of modulation depths, the three setups will measure the same nonlinearity, and all of them can be interchanged.